PHYSOR 2012 – Advances in Reactor Physics – Linking Research, Industry, and Education
Knoxville, Tennessee, USA, April 15-20, 2012, on CD-ROM, American Nuclear Society, LaGrange Park, IL (2012)

STABILITY AND CONVERGENCE ANALYSIS OF THE QUASI-DYNAMICS METHOD FOR THE INITIAL PEBBLE PACKING

Yanheng Li and Wei Ji*
Department of Mechanical, Aerospace and Nuclear Engineering
Rensselaer Polytechnic Institute
110 8th Street, JEC 5040 MANE, Troy, NY 12180
liy19@rpi.edu; jiw2@rpi.edu

ABSTRACT

The simulation for the pebble flow recirculation within Pebble Bed Reactors (PBRs) requires an efficient algorithm to generate an initial overlap-free pebble configuration within the reactor core. In the previous work, a dynamics-based approach, the Quasi-Dynamics Method (QDM), has been proposed to generate densely distributed pebbles in PBRs with cylindrical and annular core geometries. However, the stability and the efficiency of the QDM were not fully addressed. In this work, the algorithm is reformulated with two control parameters and the impact of these parameters on the algorithm performance is investigated. Firstly, the theoretical analysis for a 1-D packing system is conducted and the range of the parameter in which the algorithm is convergent is estimated. Then, this estimation is verified numerically for a 3-D packing system. Finally, the algorithm is applied to modeling the PBR fuel loading configuration and the convergence performance at different packing fractions is presented. Results show that the QDM is efficient in packing pebbles within the realistic range of the packing fraction in PBRs, and it is capable in handling cylindrical geometry with packing fractions up to 63.5%.

Key Words: Pebble Bed Reactors, Sphere packing, Packing fraction, Contact force

1. INTRODUCTION

As the next generation high temperature pebble bed reactor (PBR) designs, the Very High Temperature Gas-cooled Pebble Bed Reactor (VHTR-PBR) and the Fluoride-salt High-Temperature Reactor (FHR) have received much attention due to the good fuel economy, management and safety feature. In PBRs, the fuel pebbles circulate within the reactor core while the helium or fluoride-salt coolant passes through the fuel pebble assembly [1-3]. The accurate simulation of the coupled pebble-coolant flow can provide reliable predictions and decisions for the PBR operations. As the first step in the simulation, an initial pebble configuration is needed [4,5]. This step can be viewed as a random packing problem with mono-sized hard spheres densely arranged within a confined space (usually a container).

The random sphere packing problem has been studied for a long time [6], and many numerical algorithms and strategies have been developed to solve this problem. Based on sphere generation strategy, these algorithms can be categorized as sequential or collective packing methods [7, 8]. In the sequential packing methods, spheres are added into the domain one-by-one [9], or group-

* Corresponding author, jiw2@rpi.edu Tel: +1 (518) 276 6602; Fax: +1 (518) 276 6025

by-group [8] and the non-overlapping rule is enforced throughout the insertion. In the collective packing methods, spheres are first inserted into the container allowing sphere overlap and then a collective sphere position rearrangement or sphere size adjustment is performed to eliminate the overlap [10, 11]. Although the sequential strategy usually has high efficiency and is widely adopted [8], it cannot well control the total insertions and the packing fraction, which is of necessity for the PBR application. Contrarily, collective strategy is normally not as fast and simple as the sequential one, but can adequately control the total sphere number and hence the volume packing fraction. From a physics perspective, the packing algorithm can also be divided into dynamics-based methods and non-dynamics-based methods. In the dynamics-based methods, such as the sequential gravitational deposition method [12] or the collective discrete element method (DEM) [7, 8], the realistic forces are adopted to implement the rearrangement. The resultant sphere packing configuration can be close to the realistic case [13]. However, most dynamics-based methods are not efficient and even worse when the packing approaches random close packing (RCP) state [10]. On the contrary, the non-dynamics-based methods rearrange the packing configuration by purely mathematical manipulations without any physics consideration, such as domain triangulation [8] or mathematical optimization [14] methods. They generally have better efficiency at high packing fraction range that is close to RCP. However, the realistic fidelity is normally lost. In the realistic configuration of PBRs, the pebbles are stacked at around 61%~62% volume packing fractions and some real forces exist between pebbles and pebble-to-walls. In order to provide an initial packing configuration that has the similar packing fractions as the realistic configuration and has accounted for the actual physical forces, a collective dynamics-based method is needed for the PBR initial pebble packing.

In the previous work [13], the Quasi-Dynamics Method (QDM), a collective dynamics-based method, has been developed to generate an initial pebble packing in PBRs. In the proposed method, the positions of the predetermined number of pebbles are first generated by the uniform sampling allowing pebble overlaps. Then an efficient overlap elimination process is applied based on a simplified normal contact force model. It has shown that the developed method can successfully provide fast packing for a PBR design including the cylindrical and annular core geometries. However, the stability and the efficiency of the developed method depend on the user-defined parameters and how to choose these parameters for an optimal performance is still unknown. Besides, the packing fraction also has great influence on the algorithm convergence. These issues were not fully addressed and analyzed yet.

In this paper, the algorithm is reformulated into a two-parameter form, and the impact of these two control parameters on the algorithm performance is analyzed through two extreme 1-D cases which represent the smallest and largest close packing situations. And then the conclusion from 1-D situation is extended and verified numerically for 3-D case. For the packing fraction impact, the numerical results show that the QDM works efficiently for the packing fractions below 63%, which is within the realistic PBR packing fraction range [2]. The algorithm can handle packing fractions up to 63.5%, which is approximately the random close packing (or more precisely, maximally random jamming) state [6, 15]. For packing fractions higher than this value, since local jamming widely exists, the algorithm is hard to converge. Certain techniques, such as vibration, are needed to shift the spheres out of the jammed state.

2. THE QUASI-DYNAMICS METHOD (QDM)

In the Quasi-Dynamics Method (QDM), the basic idea is regarding the pebble-to-pebble overlap as a compressed spring system. After all the pebbles are initially positioned by uniformly sampling each pebble's center position in the PBR core region, overlaps between pebbles exist due to the finite size of pebbles. A pebble bears repulsive forces from all other overlapped pebbles. Each force points to the center of the pebble in question along the center-to-center direction and its magnitude is determined by the overlap size. The total net repulsive force, summation of each repulsive force from overlapped pebbles, determines the direction and the distance to move the pebble. In the QDM, the moving distance is assumed proportional to the magnitude of the total net force. During the overlap elimination, if a pebble overlaps with the pebble bed wall, the wall-to-pebble repulsive force is calculated in a similar way. The general procedure of the QDM has been described in the previous paper [13] and is summarized below:

For two overlapped pebbles i and j, located at $\boldsymbol{X}_i$, $\boldsymbol{X}_j$, with radii r_i and r_j, the overlap size δ_{ij} can be defined as $r_i+r_j-\|\boldsymbol{X}_i-\boldsymbol{X}_j\|$. The repulsive force acted on pebble i is calculated by:

$$\boldsymbol{F}_{n,ij} = K_p \sqrt{r_{ij}}\,\delta_{ij}\boldsymbol{n}_{ij}, \tag{1}$$

where $r_{ij}= r_i r_j/(r_i+r_j)$, K_p is a constant associated with the pebble elastic constant, and $\boldsymbol{n}_{ij}$ is a unit normal vector defined as $(\boldsymbol{X}_i-\boldsymbol{X}_j)/\|\boldsymbol{X}_i-\boldsymbol{X}_j\|$. If there are M pebbles that overlap with pebble i, the total repulsive force $\boldsymbol{F}_i$ acting on pebble i is the vector summation of $\boldsymbol{F}_{n,ij}$ over all M pebbles:

$$\boldsymbol{F}_i = \sum_{j=1}^{M} \boldsymbol{F}_{n,ij} = \sum_{j=1}^{M} K_p \sqrt{r_{ij}}\,\delta_{ij}\boldsymbol{n}_{ij}. \tag{2}$$

Similarly, if a pebble overlaps with the wall boundary and the overlap size is δ_{wi}, the repulsive wall-to-pebble contact force $\boldsymbol{W}_i$ is calculated by:

$$\boldsymbol{W}_i = K_w \sqrt{r_i}\,\delta_{wi}\boldsymbol{n}_{wi}, \tag{3}$$

where K_w is a constant associated with the wall elasticity, and $\boldsymbol{n}_{wi}$ is the wall's outer unit normal vector.

The displacement of the pebble is calculated by:

$$\Delta\boldsymbol{X}_i = K_v\left(\boldsymbol{F}_i + \boldsymbol{W}_i\right)\Big/ r_i^3 = K_v\left(\sum_{j=1}^{M} K_p\sqrt{r_{ij}}\,\delta_{ij}\boldsymbol{n}_{ij} + K_w\sqrt{r_i}\,\delta_{wi}\boldsymbol{n}_{wi}\right)\Big/ r_i^3, \tag{4}$$

where K_v is a constant determined by users.

In the QDM, one iteratively performs the overlap elimination process for every pebble based on Eqs. (1)-(4) until no overlap exists. The optimal convergence performance can be obtained by adjusting the constants K_p, K_w, and K_v. However, how to select these constants to 1) guarantee

the convergence, and 2) obtain the best convergence rate, remains unknown and is the major task in this paper.

To simplify the analysis, we only analyze the system packed with the mono-sized spheres, which is the typical PBR configuration.

For mono-sized sphere system, r_i and r_{ij} become constants, Eq. (4) can be further simplified as:

$$\Delta \boldsymbol{X}_i = \alpha \left(\sum_{j=1}^{M} \delta_{ij} \boldsymbol{n}_{ij} + \beta \delta_{wi} \boldsymbol{n}_{wi} \right), \tag{5}$$

where α and β are two control parameters that determine the algorithm stability and efficiency. α is a measure of the moving distance, i.e. step size at each iteration and β is the relative wall-to-pebble stiffness. In practice, the value of β is set to be greater than 2 to make sure the wall has higher repulsive force than the pebbles so the pebbles are more easily pushed to the core region. By using α and β, it equivalently simplifies the pebble-to-pebble repulsive force as:

$$\boldsymbol{F}_{n,ij} = \delta_{ij} \boldsymbol{n}_{ij}, \tag{6}$$

and the wall-to-pebble repulsive force as:

$$\boldsymbol{W}_i = \beta \delta_{wi} \boldsymbol{n}_{wi}. \tag{7}$$

When the QDM is applied to packing pebbles in the PBR, two quantities can be used as the convergence criterion: the maximum overlap and the average overlap at each step of the iteration. In general, these two quantities may present oscillating behavior as the iteration step k increases, which will be shown in the later sections. As long as the step-average values of these two quantities decrease as k increases, the algorithm is convergent. Otherwise, the algorithm is not stable (divergent) or stabilizes at a jamming state without leading to overlap free configuration. In practice, it is found that the algorithm stability and convergence performance is not only determined by the control parameters α and β, but also related to the system packing fraction, geometry size, and the initial pebbles' distribution (initial overlaps) by the uniform sampling. Due to these complications, it is impossible to precisely derive the range of the control parameters in which the QDM is convergent. However, by studying some 1-D sphere packing systems, which represent some typical extreme packing states in 3-D cases, some strict analytical relationship can be derived and may provide insightful understanding of the algorithm for better performance in the 3-D packing systems.

In the following sections, the impact of the control parameters (especially α) on the QDM stability and efficiency will be discussed for 1-D and 3-D packing systems via the theoretical and numerical approaches. Furthermore, the impact of the packing fraction on the QDM convergence is also presented through numerical analysis by using a "system energy" concept.

3. STABILITY ANALYSIS OF THE QDM

The control parameters α and β are not independent with each other and both affect the algorithm convergence and efficiency. For convenience, we fix the value of β and study the impact from α. It will show later that a relationship between α and β can be obtained so the impact from β can be automatically obtained. For a general packing system, it is expected that the algorithm efficiency will be enhanced as α is increased since most overlaps can be eliminated quickly. However, if α is too large, it may cause more overlaps generated than the previous step, so causing the low efficiency or a divergence. A critical value α_c is expected to exist such that the QDM is unstable if $\alpha>\alpha_c$. In order to find out this critical value for the sphere packing system, two simple extreme 1-D close packing systems are studied. Both systems can just allow two spheres packed horizontally without overlaps. One is a fixed boundary system, which corresponds to the smallest 1-D constrained multi-sphere packing system assuming that spheres can only be packed horizontally. The other one is a periodic boundary system, which corresponds to the largest 1-D system with infinite spheres packed horizontally in the infinite system. If the QDM is applied to pack spheres in these systems given an arbitrary initial packing with overlaps, how the parameters α and β affect the convergence to the overlap free configurations and what is the critical value α_c can be answered analytically.

Figure 1(a) shows the fixed boundary system. Assume that two spheres are initially packed symmetrically around the center of the system and have a small overlap $\delta_0=\delta^{(0)}=0.1r$, where r is the sphere radius.

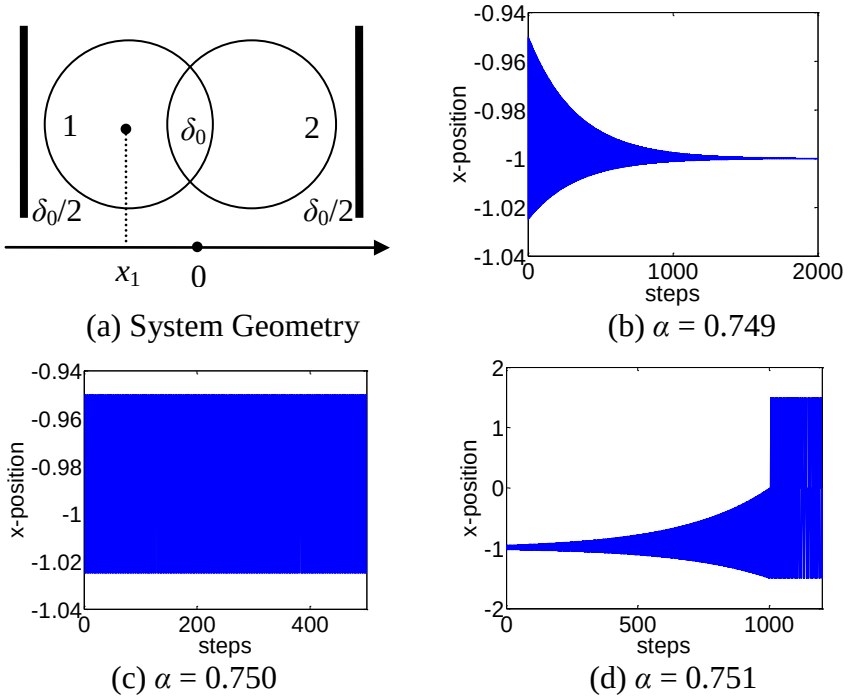

(a) System Geometry (b) α = 0.749

(c) α = 0.750 (d) α = 0.751

Figure 1. Sphere motion with respect to different α (Fixed Boundary)

Due to symmetry, both spheres have a distance of $\delta^{(0)}/2$ to the boundary. The critical value α_c can be obtained by analyzing sphere 1's consequent motions by the QDM. The initial position for

sphere 1 is $x_1^{(0)}$=-r+δ_0/2. Assume that α is large enough (>1/2), after the first step, sphere 1 is moved to an updated position $x_1^{(1)}$=-r+(1/2-α)δ_0 and the overlap between two spheres disappears. However, new overlap with the left wall (boundary) appears: $\delta_{1w}^{(1)}$=(α-1/2)δ_0. This wall-to-sphere overlap would push the sphere 1 to move rightward to the new position: $x_1^{(2)}$=-r+($\beta\alpha$-1)(1/2-α)δ_0 and new overlap between two spheres appear. If the algorithm is convergent, it is required that the new overlap be smaller than the initial overlap, therefore it has $x_1^{(2)}<x_1^{(1)}$. After simple calculation, one obtains:

$$\alpha < \alpha_c = \frac{1}{\beta} + \frac{1}{2}. \tag{8}$$

Eq. (8) provides a stability range for the parameter α, meanwhile, it sets up the relationship between the parameter β and the critical value α_c. If $\alpha<\alpha_c$, the system is convergent. If $\alpha=\alpha_c$, the system is stable but not convergent. Both spheres will move back and forth with the displacement of $\alpha\delta_0$ and the overlap is constant. If $\alpha>\alpha_c$, two spheres will swap position or even have infinite displacement no matter how small δ_0 is, hence the system is unstable. Figures 1(b)-(d) show these behaviors during the packing at the values of β=4 and α_c=0.75. These results directly verify the prediction by Eq. (8). Also, Eq. (8) implies that greater β (relative wall-to-sphere stiffness) leads to smaller value of α_c. This can be understood by noting that a harder wall can bounce the sphere back further to cause larger overlaps with other spheres if α is too large. A small value of α can prevent such a large displacement from the wall so the stability range of α becomes smaller.

It should be noticed that Eq. (8) is derived from a strictly close 1-D packing case. For a loose packing, a higher α_c is expected, and for a denser packing, a lower α_c is expected. Figure 2 shows two examples for a loose packing and a denser packing, respectively, where ε is a small positive number. By following similar procedure that derives Eq. (8) , we find α_{c1}=1/β+0.5-δ_0/(4r) for Figure 2(a), and α_{c2}=1/β+0.5+ε for Figure 2(b). Note that the denser packing case shown in Figure 2(a) represents a local jamming packing situation that could happen in a real packing system. A smaller range of α can be chosen for denser packing cases.

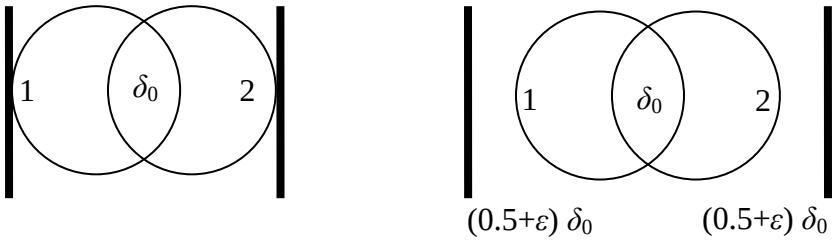

(a) Denser packing (b) Loose packing

Figure 2. Denser packing and loose packing situations

The critical step size value for the periodic boundary 1-D system can also be determined following the similar procedure as the fixed boundary system. Figure 3(a) shows the system configuration, which corresponds to an infinite close packing system. Under periodic boundary conditions (PBC), only sphere-to-sphere overlap exists, hence the parameter β has no impact on

the algorithm performance. By using the same approaches that derives Eq. (8), one can obtain the critical value of α_c for the PBC system:

$$\alpha_c = 1, \tag{9}$$

which is numerically verified by Figure 3(b)-(d).

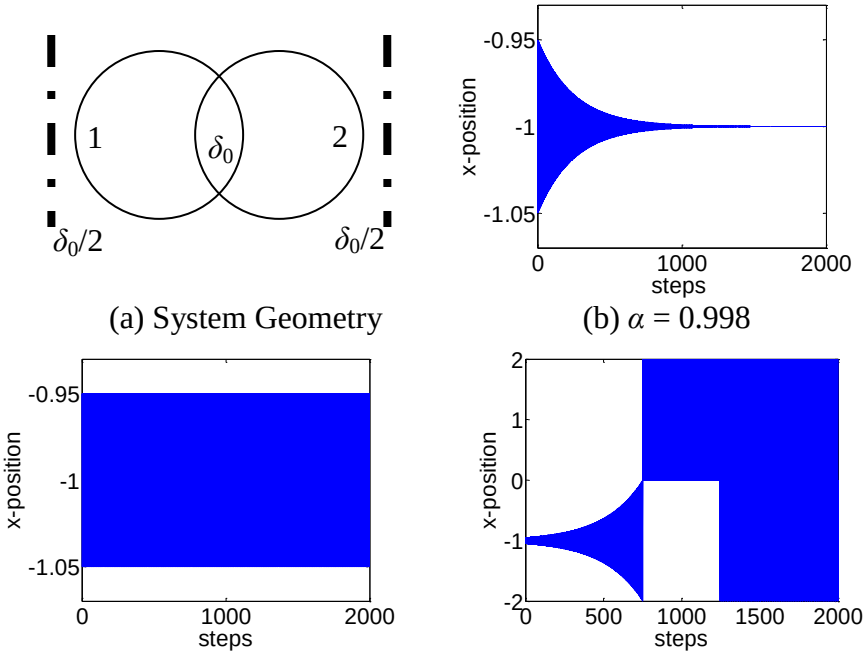

(a) System Geometry (b) α = 0.998

(c) α = 1.000 (d) α =1.002

Figure 3. Position history of sphere 1 under PBC

Now it can be concluded that, for close packing in finite 1-D geometry which lies between Figures 1(a) and 3(a), there should be $\alpha < \alpha_c \in (0.5 + 1/\beta, 1)$ exists to guarantee the stability of the algorithm. For large system which is close to the periodic boundary condition, $\alpha_c \to 1$, so α can be chosen closer to 1.

For 3-D system, it is hard to obtain exactly quantitative influence of control parameters on the algorithm performance. However, the 3-D system does share some similarities with the 1-D system just studied. Specifically, the value of α_c in closely packed 3-D system is also expected to lie within the range of (1/2+1/β, 1). A numerical experiment for cylinder geometry packing is performed to verify this upper limit for α. The geometry of the problem originated from HTR-10 configuration [16]: the cylindrical core has a height H_c=180cm and radius R_c=90cm, as shown in Figure 4(a). A total of about 24726 spheres are packed inside the core with the sphere radii at r=3cm, which has a packing fraction of *frac*=0.61. The stop criterion is chosen as the maximum overlap less than $r/10^5$. It costs about 150 seconds for every 1000 steps on a Pentium IV 3GHz CPU PC.

Figure 4(b) shows the impact of α and β on the iteration steps. The right end of each curve corresponds to α_c. It can be observed that, as expected, the algorithm efficiency increases as α increases. Also an increase in the β value leads to the faster overall convergence but smaller α_c, which is consistent with the prediction by Eq. (8). For fixed β, optimal α^* exists as α approaches α_c. For the 61% packing shown in Figure 4, there are about 20k contacting sphere pairs and only 0.6k wall contacts, therefore this packing is close to the infinite geometry, which accounts for the fact that α_c is close to 1. In practice, in order to achieve high efficiency, the value of α should be set close to α_c.

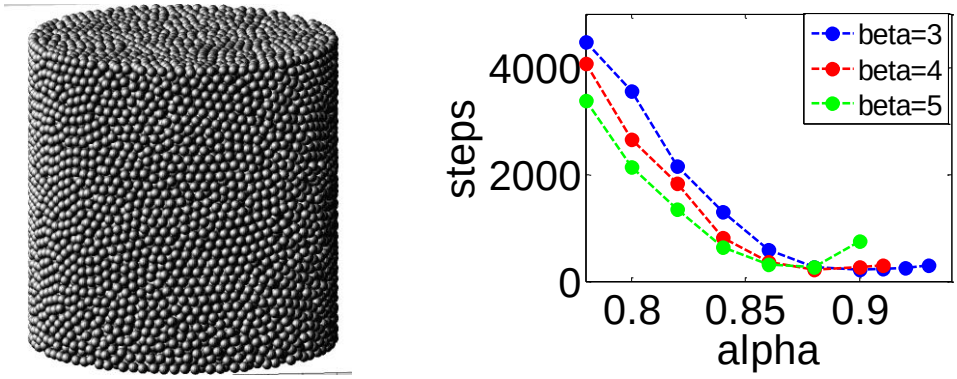

(a) Cylindrical geometry (b) Parameter impact on convergence

Figure 4. Impacts of the control parameters on the QDM convergence performance

4. PACKING FRACTION IMPACT ON THE QDM CONVERGENCE

From Section 3, it shows that the packing fraction *frac* also has notable impact on the QDM convergence, especially when the system is close to the random close packing state, where sphere jamming may occur. Sphere jamming will significantly deteriorate the convergence performance. For example, Figure 5 shows a possible scenario of the jammed state when three spheres are packed in a 3-D system. When the QDM is applied to pack these three spheres, at some point, they may line up along the line A, even if the control parameters are chosen less than critical values. There are overlaps existing for these spheres, but since $\boldsymbol{F}_i+\boldsymbol{W}_i=0$ for any sphere i, QDM will not able to proceed and all the three spheres will stay still. The QDM is considered still stable but not convergent. In this case, a random vibration is needed to shift the system out of this jammed state. Such a jammed state is related to the system packing fraction. The closer to the random close packing, the more possible the jammed state occurs.

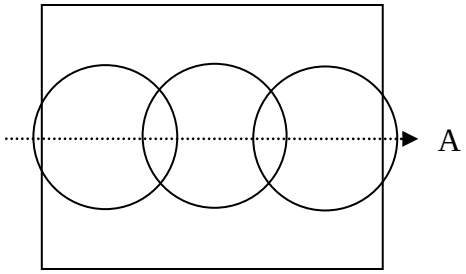

Figure 5. Jammed packing state

In order to form a quantitative view of this impact, mono-sized sphere packing in a cylinder with four different packing fractions are investigated. The system geometry is the same as shown in Figure 4(a). In all the four cases, α is set to be 0.86, which is around the optimal performance value, and β is set to be 4. To observe the algorithm performance during the packing, besides the step-dependent maximum overlap and average overlap, a convergence rate defined using a "system energy" concept at each step is introduced to quantitatively describe the QDM convergence efficiency.

As described at the beginning of Section 2, the overlap is regarded as a compressed spring system. It can be assumed that certain "potential energy" is stored for each overlap. During the iteration, the overlaps for each pebble are changing so the total "potential energy" for the packing system is changing. If the total "potential energy" has a global decrease behavior as the overlap elimination is performed iteratively, the algorithm is considered convergent. When overlaps are completely eliminated, the total "potential energy" becomes zero. This energy concept can help analyze and understand the stability and convergence of the QDM. Based on the linear contact repulsive force model described in Eqs. (6) and (7), the step-dependent total "potential energy" for the packing system can be defined as:

$$\begin{aligned} V^{(k)}(\boldsymbol{X}^{(k)}) &= \frac{1}{2}\left(\sum_{i=1}^{N}\sum_{j=1}^{M} F_{\mathrm{n,ij}}^{(k)}\delta_{\mathrm{ij}}^{(k)} + \sum_{i=1}^{N} W_{\mathrm{i}}^{(k)}\delta_{\mathrm{wi}}^{(k)} \right) \\ &= \frac{1}{4}\sum_{i=1}^{N}\sum_{j=1}^{M}\left(\delta_{\mathrm{ij}}^{(k)}\right)^2 + \frac{1}{2}\beta\sum_{i=1}^{N}\left(\delta_{\mathrm{wi}}^{(k)}\right)^2 \\ &\geq 0. \end{aligned} \tag{10}$$

When the system is overlap free, the total "potential energy" becomes 0, i.e. $V(\boldsymbol{X}^*) = 0$. Therefore $V(\boldsymbol{X})$ can be used to measure the overall overlap of the system. Convergence rate for k^{th} step can be characterized as:

$$\rho^{(k)} = \frac{V^{(k)}(\boldsymbol{X})}{V^{(k-1)}(\boldsymbol{X})}. \tag{11}$$

If the QDM is convergent, then the average value of the convergence rate $\bar{\rho} < 1$ as $k \to \infty$.
Figure 6 shows the QDM convergence behavior at the packing fractions of 58%, 61%, 62.5%, and 63.5%. The maximum and average overlap sizes, as well as the convergence rate defined by Eq. (11) are plotted as the function of the iteration step k.

From Figure 6, it can be seen that, for a large cylindrical geometry, QDM can handle the packing fraction up to 63.5%, which approximately corresponds to the random close packing (maximum jamming state). For the loose packing at 58% and 61%, shown in Figures 6 (a) and (b), the convergence criterion (ρ<1) can be strictly satisfied for every step. As packing fraction increases above 62.5%, local jamming starts to form, and ρ will be greater than 1 occasionally. However, since the average convergence rate $\bar{\rho}$ is less than 1, the system can still converge to an overlap-free configuration. As for high density packing (*frac*>63.5%), where local jamming widely exists

and $\bar{\rho} > 1$, the QDM will fail to proceed and multiple vibrations are needed to shift the spheres out of jammed state.

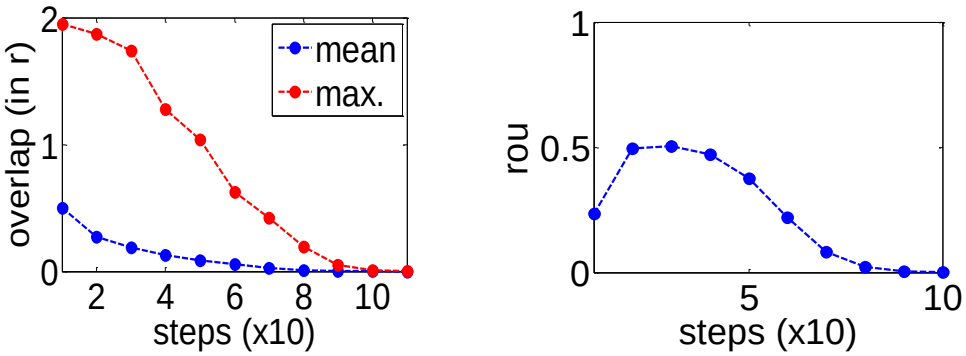

(a) *frac*=0.58

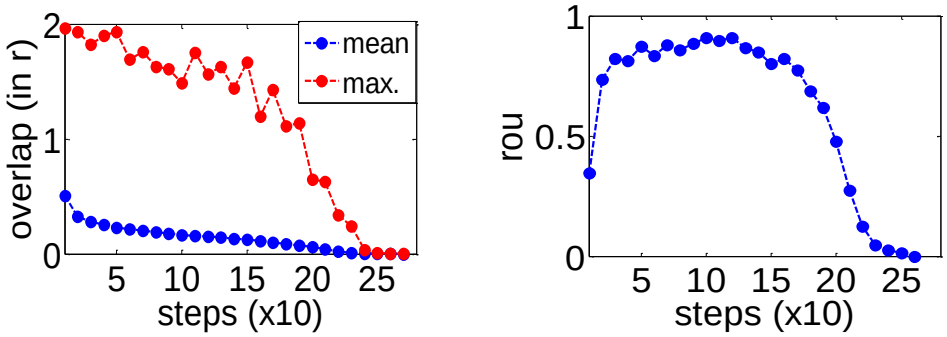

(b) *frac*=0.61

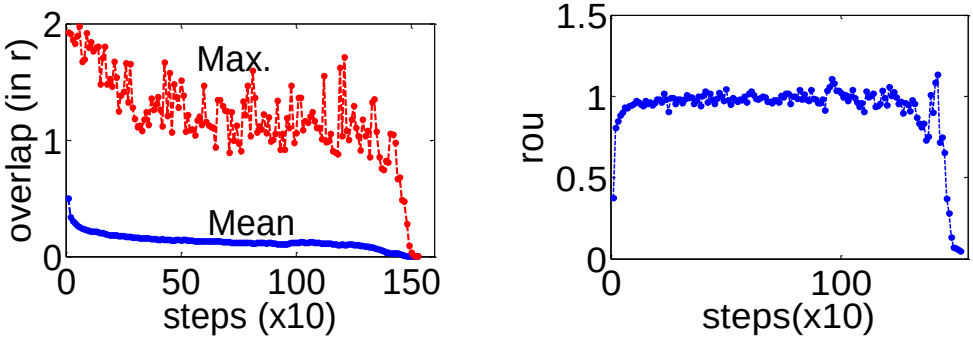

(c) *frac*=0.625

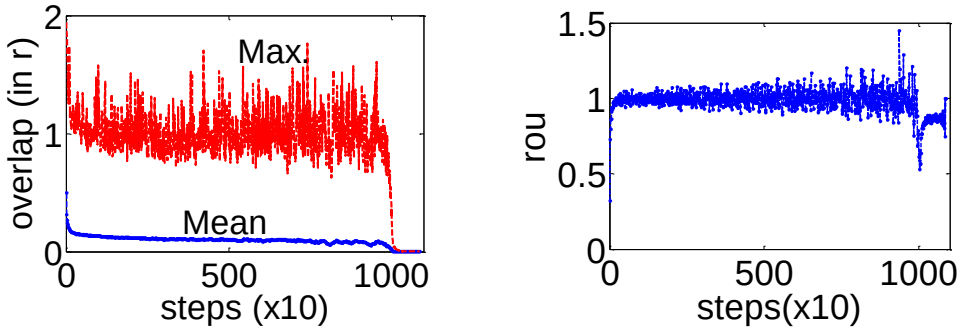

(d) *frac*=0.635

Figure 6. QDM convergence performance for different packing fractions

5. CONCLUSIONS

The original Quasi-Dynamics Method (QDM) is reformulated into a simplified version with two control parameters, the relative wall-to-sphere stiffness β and the step size α. Analytical results from extreme 1-D situations show that for fixed β, the step length has a range within $(1/2+1/\beta,1)$. Since for the 3-D situation, it is difficult to obtain similar analytical estimations, a numerical analysis is performed to verify the prediction that the step size α should still lie within the same range. Due to the large size of the Pebble Bed Reactor core (container) geometry, the upper limit for α is close to the infinite geometry situation, where α_c=1. The most important conclusion from the numerical 3-D analysis is that, in order to achieve high efficiency, α should be close to α_c. The impact of β is also investigated, which shows that larger β leads to a smaller α_c, which agrees with the simulation results from the 1-D prediction.

The algorithm is applied to the PBR applications with different packing fractions. The convergence performance shows that the algorithm can handle packing fractions as high as 63.5%, which is around the random close packing limit. For packing fractions higher than that, due to the widely existence of local jamming or even strict global jamming, QDM is hard to proceed and other auxiliary techniques, such as vibration, are needed to shift the system out of the jamming state.

REFERENCES

1. E. Teuchert, H. J. Rutten, "Core Physics and fuel cycles of the pebble bed reactor," *Nuclear Engineering and Design*, **34**, pp.109-118 (1975).
2. C. H. Rycroft, et al., "Analysis of granular flow in a pebble-bed nuclear reactor," *Physical Review E*, **74**, 021306 (2006).
3. C. W. Forsberg, P. F. Peterson, and R. A. Kochendarfer, "Design Options for the Advanced High-Temperature Reactor," *Proceedings of ICAPP '08,* Anaheim, CA USA, June 8–12 (2008).
4. Y. Li and W. Ji, "Pebble Flow Simulation Based on a Multi-Physics Model," *Trans. Am. Nucl. Soc*., **103**, pp.323-325 (2010).
5. Y. Li and W. Ji, "Modeling of Interactions between Liquid Coolant and Pebble Flow in AHTR," *Trans. Am. Nucl. Soc*., **104**, 404-406 (2011).
6. S. Torquato, et al., "Is Random Close Packing of Spheres Well Defined?" *Phys. Rev. Lett.*, **84**, 2064-2067(2000).
7. A. M. Ougouag, et al., "Methods for modeling the packing of pebble bed reactors," *Proceedings of International Conference on Mathematics and Computation, Supercomputing, Reactor Physics and Nuclear and Biological Applications*, Avignon, France, Sept 12-15 (2005).
8. K. Bagi, "An algorithm to generate random dense arrangements for discrete element simulations of granular assemblies", *Granular Matter*, **7**, pp.31-43 (2005).
9. D. W. Cooper, "Random-sequential-packing simulations in three dimensions for spheres," *Physical Review A*, **38**, No. 1 (1988).

10. A. S. Clarke and J. D. Wiley, "Numerical simulation of the dense random packing of a binary mixture of hard spheres: Amorphous metals," *Physical Review B*, 35, NO. 14 (1987).
11. W. S. Jodrey and E. M. Tory, "Computer simulation of close random packing of equal spheres," *Physical review A*, **32**, No.4 (1985).
12. G. E. Mueller, "Numerically packing spheres in cylinders," *Powder technology*, **159**, pp.105-110 (2005).
13. Y. Li and W. Ji, "A Collective Dynamics-based Method for Initial Pebble Packing in Pebble Flow Simulation," *Proceeding of International Conference on Mathematics, Computational Methods & Reactor Physics (M&C 2011)*, Rio de Janeiro, Brazil (2011).
14. A. Sutou, et al., "Global Optimization Approach to Unequal Sphere Packing Problems in 3D," *J. of Optimiztion Theory and Applications*, **14**, pp.671-694(2002).
15. G. D. Scott and D. M. Kilgour, "The density of random close packing of spheres," *Journal of Physics D: Applied Physics*, **2**, No. 6 (1969).
16. Z. Gao and L. Shi, "Thermal Hydraulic Calculation of the HTR-10 for the Initial and Equilibrium Core," *Nuclear Engineering and Design*, **218**, pp.51-64(2002).